Development of transverse flow from the free-streaming to the hydrodynamic regime in conformal kinetic theory

Clemens Werthmann

in Collaboration with Sören Schlichting and Victor Ambruș

based on PRD 105 (2022) 014031 and WiP

Bielefeld University

CRC-TR 211
Strong-interaction matter under extreme conditions

DFG

UNIVERSITÄT BIELEFELD

HGS-HIRe for FAIR
Helmholtz Graduate School for Hadron and Ion Research

Introduction

Hadronic Collisions in Experiment

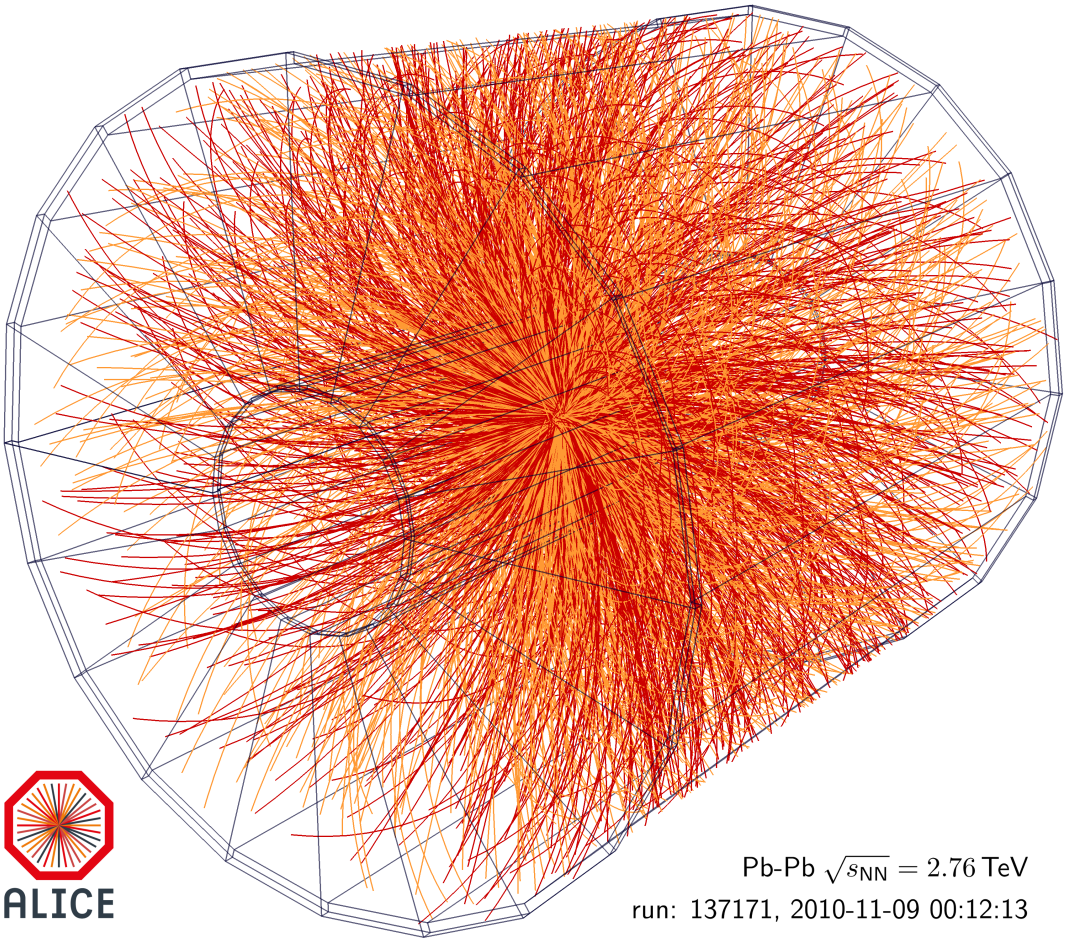

Hadronic Collisions in Experiment

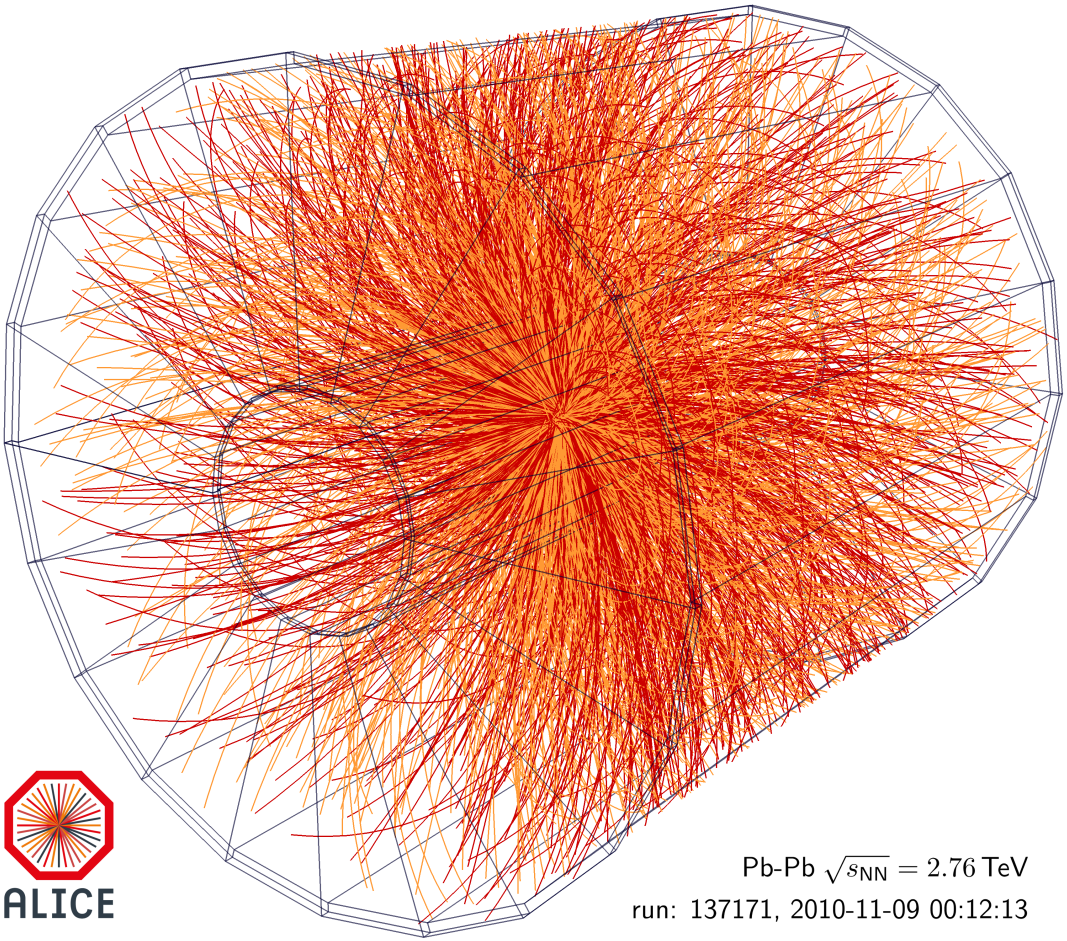

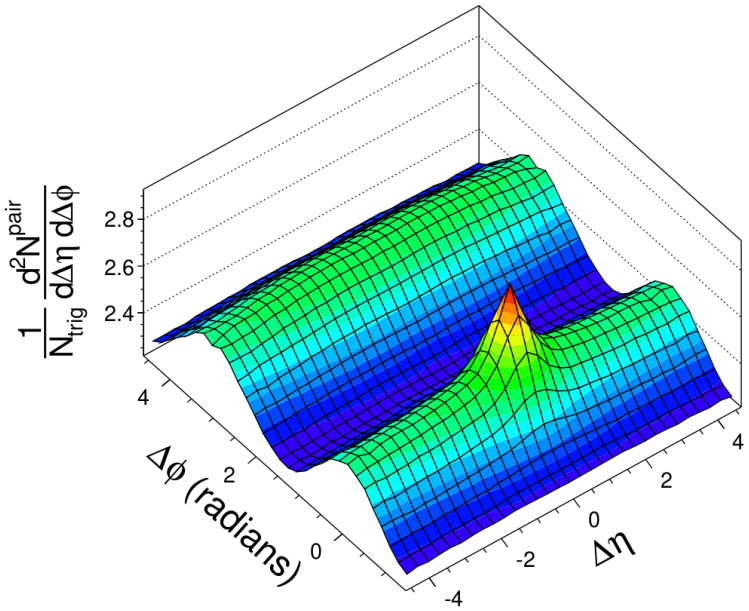

Figure (cropped): CMS Collaboration PLB 724 (2013) 213

Standard model of heavy ion collisions

Spacetime evolution dominated by hydrodynamic phase

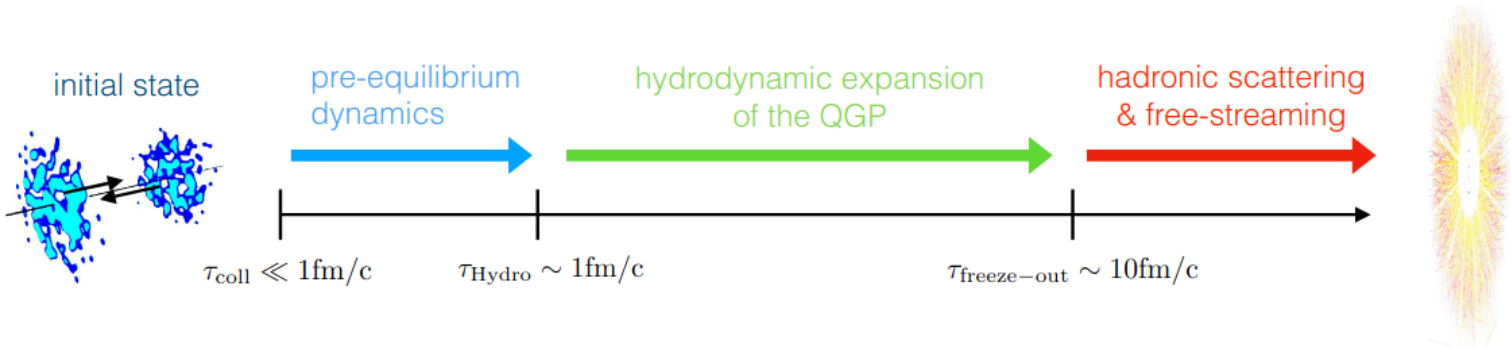

- early stage requires non-equilibrium description, but system quickly equilibrates
- strongly interacting QGP leaves imprints of thermalization and collectivity in final state observables
  - anisotropic flow explained via anisotropic pressure gradients in hydrodynamic evolution
- transport description after hadronization

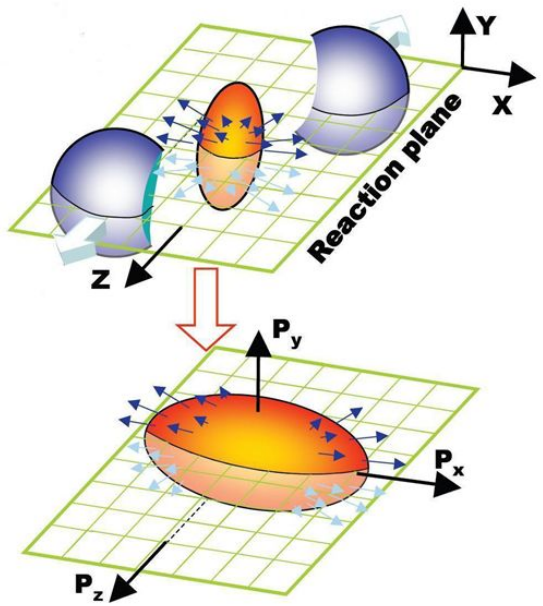

Hiroshi Masui (2008)

Small systems

Very dilute, hydrodynamics not necessarily applicable

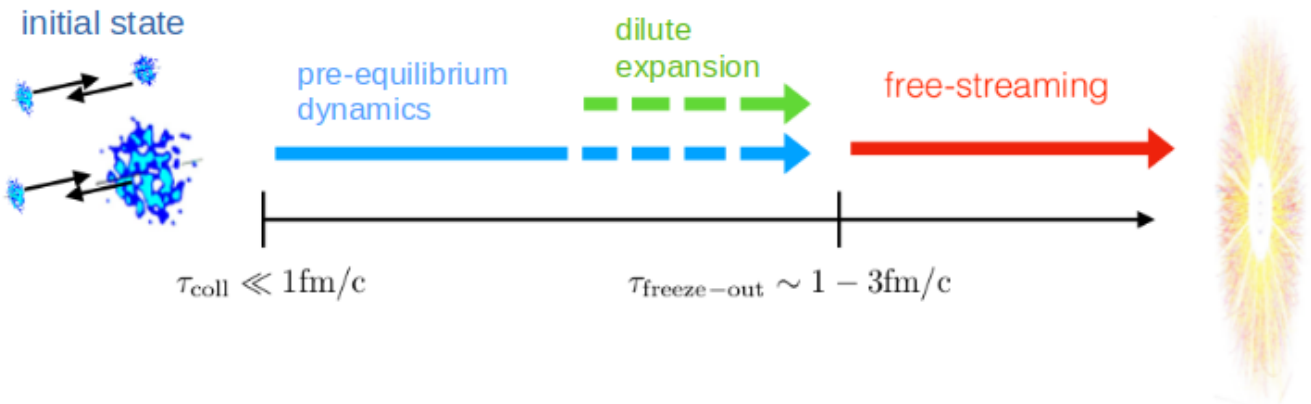

- still collective behaviour is observed!
- collectivity can also be explained in kinetic theory, a microscopic description which does not rely on equilibration
  - anisotropic flow explained via individual scatterings being more likely in some directions
- limit of large interaction rate is hydrodynamics!

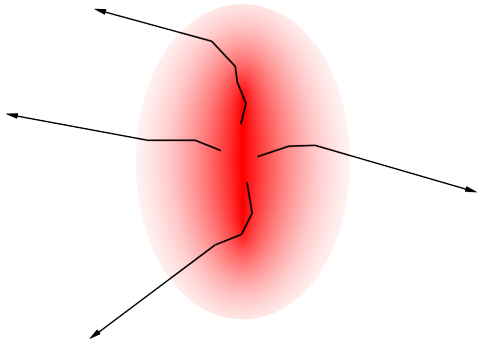

Aim

Case study in simplified kinetic theory description on full range from small to large system size with comparison to hydrodynamics based on transverse flow

Theoretical Description

- azimuthal momentum anisotropies are quantified in the "flow harmonics" defined as

$$\frac{\mathrm{d}N}{\mathrm{d}p_\perp \mathrm{d}\phi_p} = \frac{\mathrm{d}N}{2\pi \mathrm{d}p_\perp}\left(1 + 2\sum_{n=1}^{\infty} v_n(p_\perp)\cos\left[n(\phi_p - \Psi_n)\right]\right) \tag{1}$$

- models of the fireball dynamics relate the v_n to spatial anisotropies in the initial state
- strong correlation with $x_\perp^n$-weighted "eccentricities"; leading order: $v_n \propto \epsilon_n$

$$\epsilon_n = -\frac{\left\langle x_\perp^n \cos\left[n(\phi_r - \Psi_n)\right]\right\rangle_\epsilon}{\left\langle x_\perp^n \right\rangle_\epsilon}\,, \qquad \langle \mathcal{O} \rangle_\epsilon = \frac{\int_{\mathbf{x}_\perp} \mathcal{O}(\mathbf{x}_\perp)\epsilon(\mathbf{x}_\perp)}{\int_{\mathbf{x}_\perp} \epsilon(\mathbf{x}_\perp)} \tag{2}$$

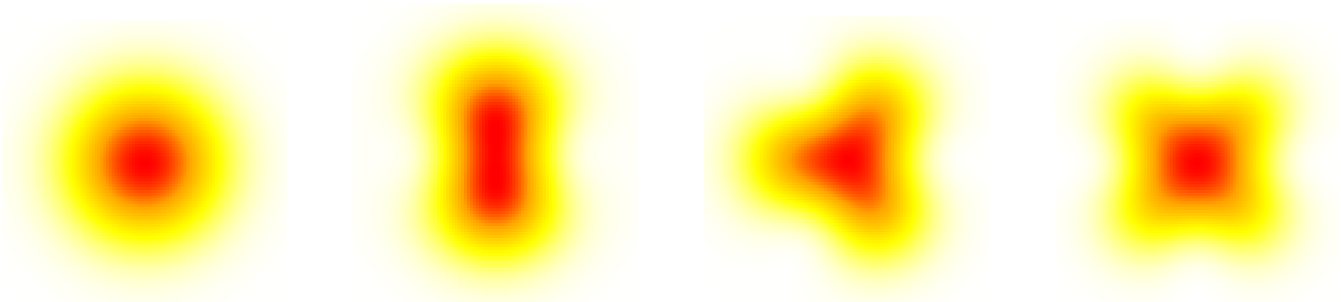

(no ecc.) $(n = 2)$ $(n = 3)$ $(n = 4)$

- microscopic description in terms of averaged on-shell phase-space distribution of massless bosons:

$$f(\tau, \mathbf{x}_\perp, \eta, \mathbf{p}_\perp, y) = \frac{(2\pi)^3}{\nu_{\text{eff}}} \frac{\mathrm{d}N}{\mathrm{d}^3x\,\mathrm{d}^3p}(\tau, \mathbf{x}_\perp, \eta, \mathbf{p}_\perp, y) \tag{3}$$

  - boost invariance: dependence only on $y - \eta$
  - initialized with vanishing longitudinal pressure and no momentum anisotropies

- time evolution: Boltzmann equation in conformal relaxation time approximation

$$p^\mu \partial_\mu f = C_{RTA}[f] = \frac{p_\mu u^\mu}{\tau_R}(f_{\text{eq}} - f)\ , \quad \tau_R = 5\frac{\eta}{s}T^{-1} \tag{4}$$

  - time evolution of f depends only on opacity $\hat{\gamma} = \left(5\frac{\eta}{s}\right)^{-1}\left(\frac{30}{\nu_{\text{eff}}\pi^2}\frac{1}{\pi}\frac{\mathrm{d}E_\perp^{(0)}}{\mathrm{d}\eta}R\right)^{1/4}$

    Kurkela, Wiedemann, Wu EPJC 79 (2019) 965
  - energy weighted d.o.f.: dependence on IS only in energy density

- first study: simple initial energy density given in analytical form, introducing only one eccentricity at a time

Analytical and numerical treatment

- typical values of $\hat{\gamma}$
  - min. bias pp: $\hat{\gamma} \approx 0.88 \left(\frac{\eta/s}{0.16}\right)^{-1} \left(\frac{R}{0.4\,\mathrm{fm}}\right)^{1/4} \left(\frac{\mathrm{d}E_\perp^{(0)}/\mathrm{d}\eta}{5\,\mathrm{GeV}}\right)^{1/4} \left(\frac{\nu_{\mathrm{eff}}}{40}\right)^{-1/4}$
  - central PbPb: $\hat{\gamma} \approx 9.2 \left(\frac{\eta/s}{0.16}\right)^{-1} \left(\frac{R}{6\,\mathrm{fm}}\right)^{1/4} \left(\frac{\mathrm{d}E_\perp^{(0)}/\mathrm{d}\eta}{4000\,\mathrm{GeV}}\right)^{1/4} \left(\frac{\nu_{\mathrm{eff}}}{40}\right)^{-1/4}$

$\Rightarrow$ treat problem both analytically (for small $\hat{\gamma}$) and numerically

linearized analytical treatment

- "opacity expansion" in number of scatterings

$$\text{0th order}: \quad p^\mu \partial_\mu f^{(0)} = 0 \,,$$

$$\text{1st order}: \quad p^\mu \partial_\mu f^{(1)} = C[f^{(0)}]$$

Heiselberg, Levy PRC 59 (1999) 2716

Borghini, Gombeaud EPJC 71 (2011) 1612

- expansion parameter $C_{\mathrm{RTA}}[f] \sim \hat{\gamma}$
- linearize also in eccentricity

numerical treatment

- nonlinear in both opacity and eccentricity
- Relativistic Lattice Boltzmann solver for energy-weighted d.o.f.

Ambrus, Blaga PRC 98 (2018) 035201

$$\mathcal{F}_{\mathrm{RLB}} \propto \int_0^\infty \mathrm{d}p^\tau \, (p^\tau)^3 f$$

Time Evolution of $T^{\tau\tau}$

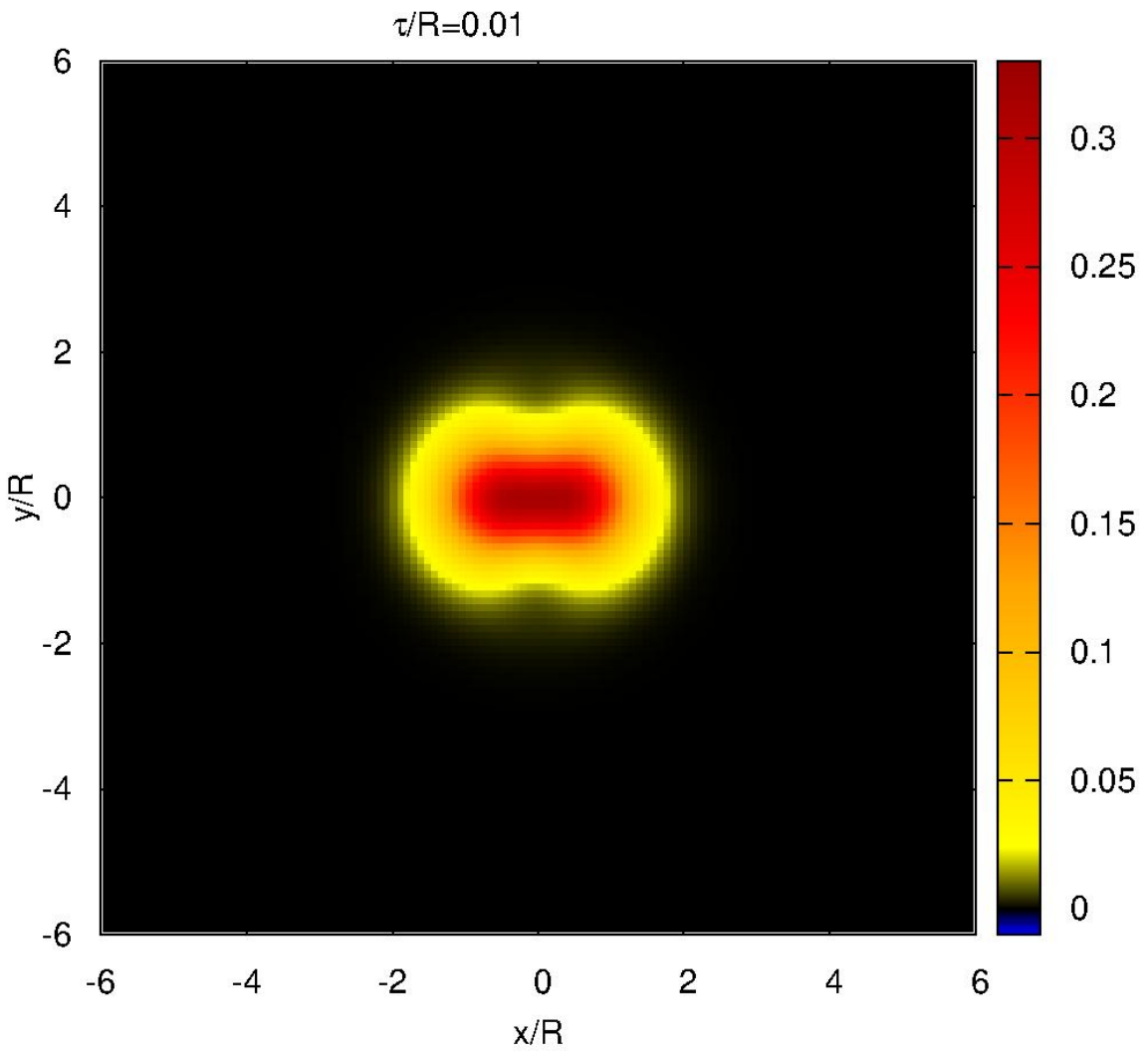

Results and Comparisons

Linear Flow Response at small $\hat{\gamma}$

linear behaviour in ϵ_n, $\hat{\gamma} \Rightarrow$ flow harmonics normalized as $v_n/(\epsilon_n\hat{\gamma})$

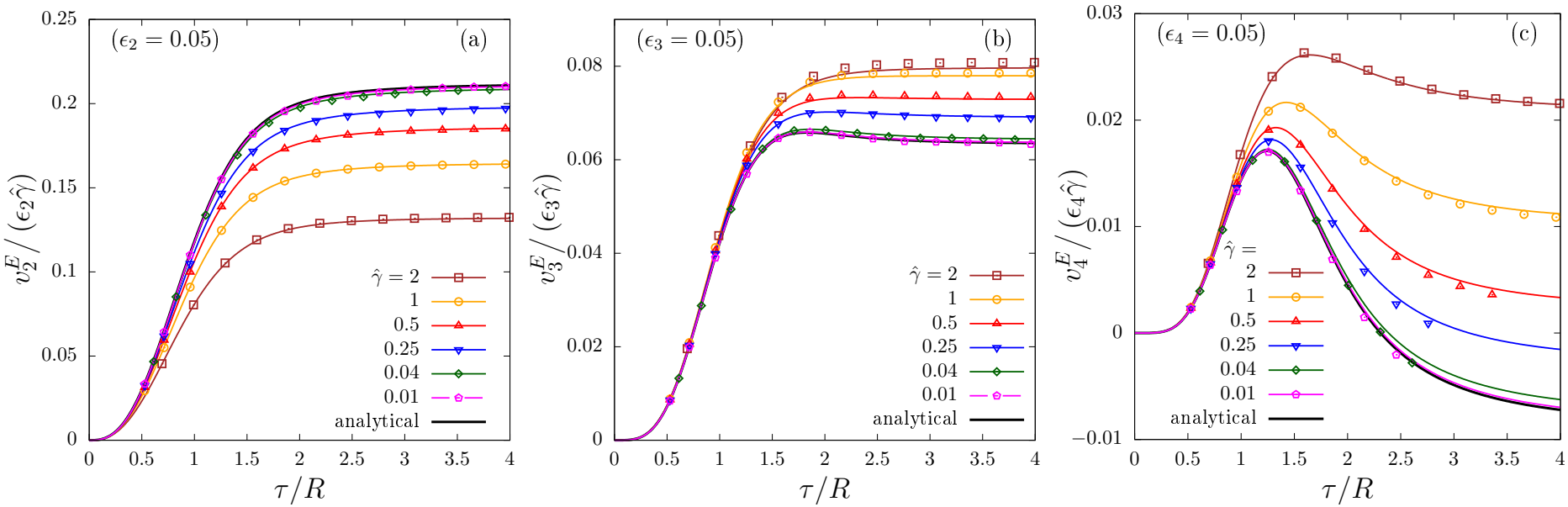

- initial buildup: $0.5 \lesssim \tau/R \lesssim 1.5$,
  $v_2/\epsilon_2 > v_3/\epsilon_3 > v_4/\epsilon_4$,
  v_4 has strong negative late time trend
- small $\hat{\gamma}$: agreement with linearized result
- larger opacities: $v_2/\hat{\gamma}$ decreases, $v_3/\hat{\gamma}$, $v_4/\hat{\gamma}$ increase

Linear Flow Resonse at large $\hat{\gamma}$

nonlinear in $\hat{\gamma} \Rightarrow$ flow harmonics normalized as v_n/ϵ_n

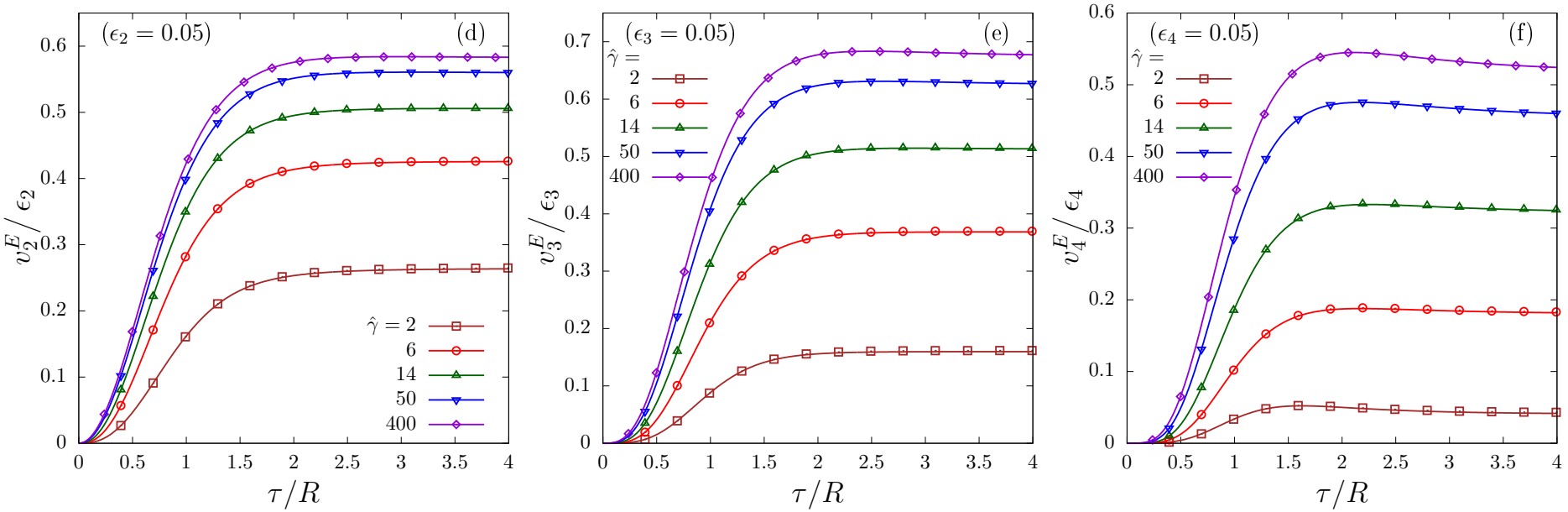

- all v_ns increase with $\hat{\gamma}$
- similar magnitudes; curves have no strong distinctive features
- transverse flow develops on timescales $\tau_\perp \sim R$
  - true also for large opacities and nonlinear responses
  - for interaction of particles coming from different parts of the initial geometry, they must cross a distance $\sim R$
- transverse expansion: $\partial_\tau f \propto \nabla_\perp f \sim 1/R \quad \Rightarrow \tau_\perp \sim R$

- cooling of the system can be measured in terms of the decrease of $\mathrm{d}E_\perp/\mathrm{d}\eta$

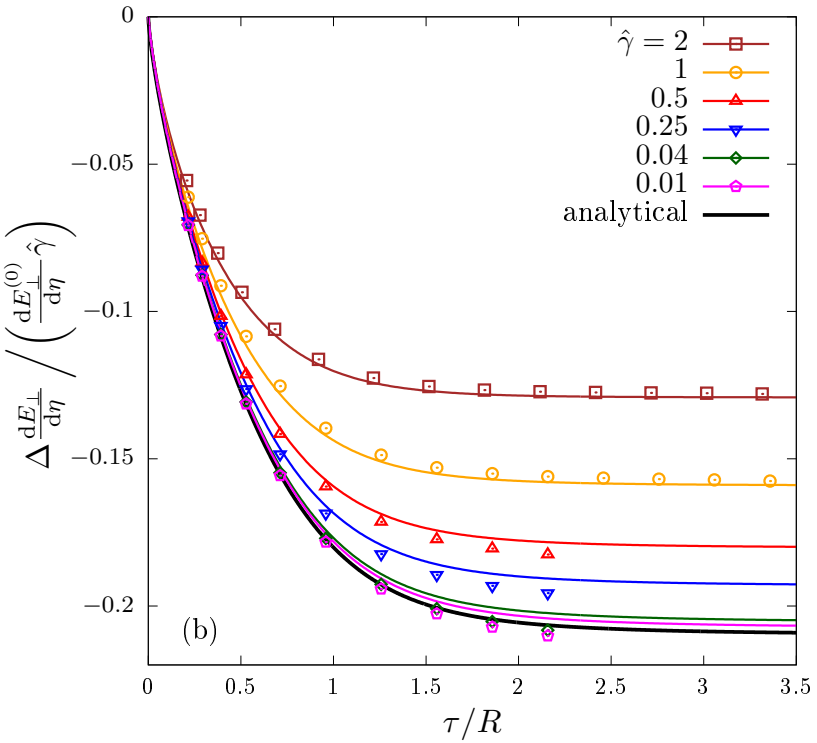

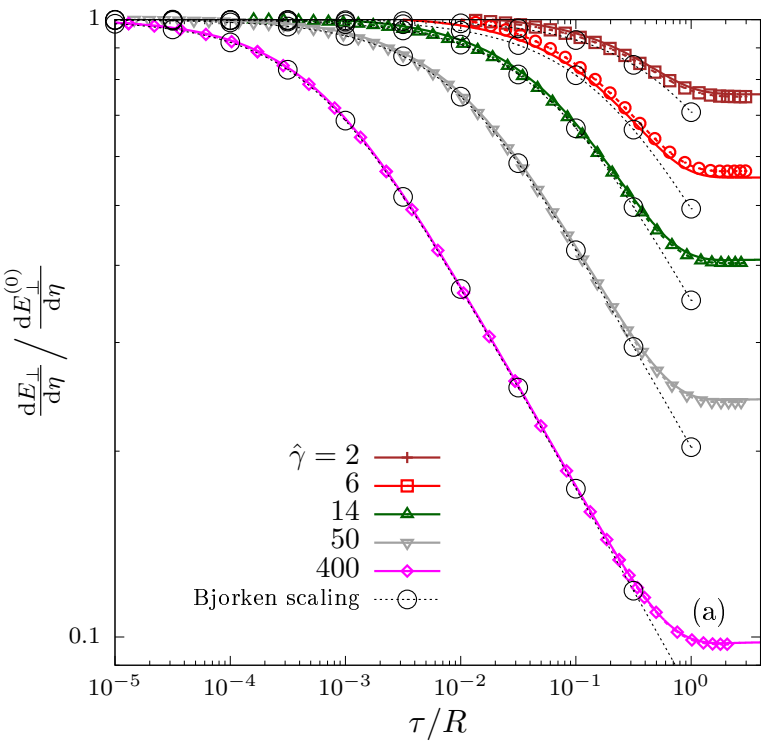

- small $\hat{\gamma}$: curves follow analytical result; for slightly larger $\hat{\gamma}$, work done per $\hat{\gamma}$ is smaller
- large $\hat{\gamma}$: curves exhibit $\propto \tau^{-1/3}$ scaling period at intermediate times, similar to Bjorken flow in 0+1D
  - can be understood using the universal Bjorken flow attractor

Bjorken flow attractor

- longitudinal boost-invariant Bjorken flow exhibits universal behaviour across different initial conditions/evolution models
- time evolution curves converge to an attractor curve when expressed via the scaling variable $\tilde{w} = \frac{T\tau}{4\pi\eta/s} \Rightarrow$ expressed via universal scaling functions $\mathcal{E}(\tilde{w}), f_{E_\perp}(\tilde{w}), ...$

Giacalone, Mazeliauskas, Schlichting, PRL 123 (2019) 262301 Ambruș, Bazzanini, Gabbana, Simeoni, Succi, Tripicione, WiP

- $\tilde{w} \gg 1$ (equilibrium): $\mathcal{E}(\tilde{w}) \propto \tau^{4/3} e = \text{const.}, \quad f_{E_\perp}(\tilde{w}) \propto \tau^{1/3} \frac{dE_\perp}{dy} = \text{const.}$
- $\tilde{w} \ll 1$: model dependent power law $\mathcal{E}(\tilde{w}), f_{E_\perp}(\tilde{w}) \sim \tilde{w}^\gamma$ (kin. theory: $\gamma = \frac{4}{9}$)

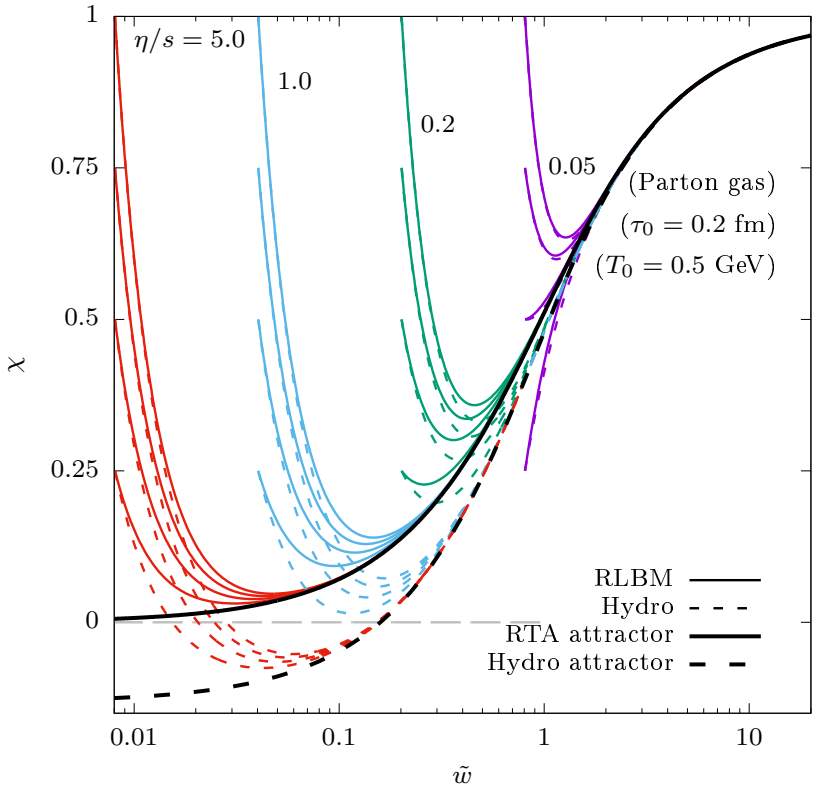

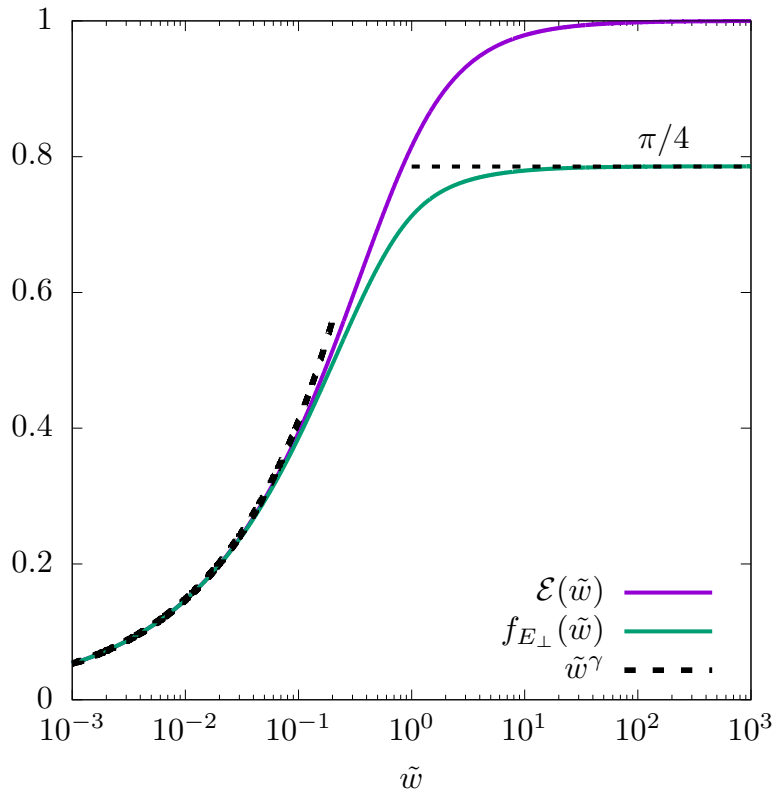

Local Bjorken flow scaling

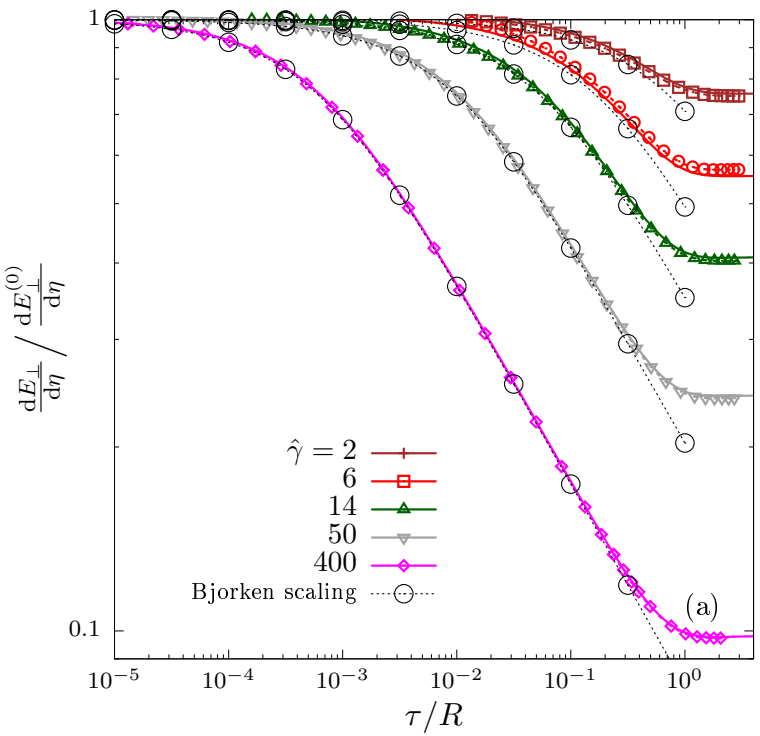

- at $\tau \ll R$, the early time cooling is dominated by longitudinal dynamics
- each part of the system does not interact with its "transverse neighbourhood" yet and can be described by local Bjorken flow scaling in the scaling variable $\tilde{w}(\tau, \mathbf{x}_\perp) = \frac{T(\tau,\mathbf{x}_\perp)\tau}{4\pi\eta/s}$

$$\tau^{1/3} \frac{\mathrm{d}E_\perp}{d^2\mathbf{x}_\perp \mathrm{d}\eta} = (4\pi\eta/s)^{4/9} a^{1/9} (\epsilon\tau)_0^{8/9} \; C_\infty \; f_{E_\perp}(\tilde{w}) \qquad (5)$$

- can use scaling to establish correnspondence $\tilde{w} \leftrightarrow \mathbf{x}_\perp$ and integrate above eq. ($\rightarrow$ grey dotted lines: accurate up to $\tau/R \sim 0.2$)
  - for large $\hat{\gamma}^{3/4}\tau$: $\frac{dE_\perp/d\eta}{dE_\perp^0/d\eta} = \frac{9\pi}{32} \left(\frac{4\pi}{5\hat{\gamma}}\right)^{4/9} \left(\frac{R}{\tau}\right)^{1/3} C_\infty$
- large $\hat{\gamma}$: time scale separation between equilibration $\tau_{\mathrm{eq}} \sim \hat{\gamma}^{-4/9} R$ and transverse expansion at $\tau_\perp \sim R$

Opacity Dependence

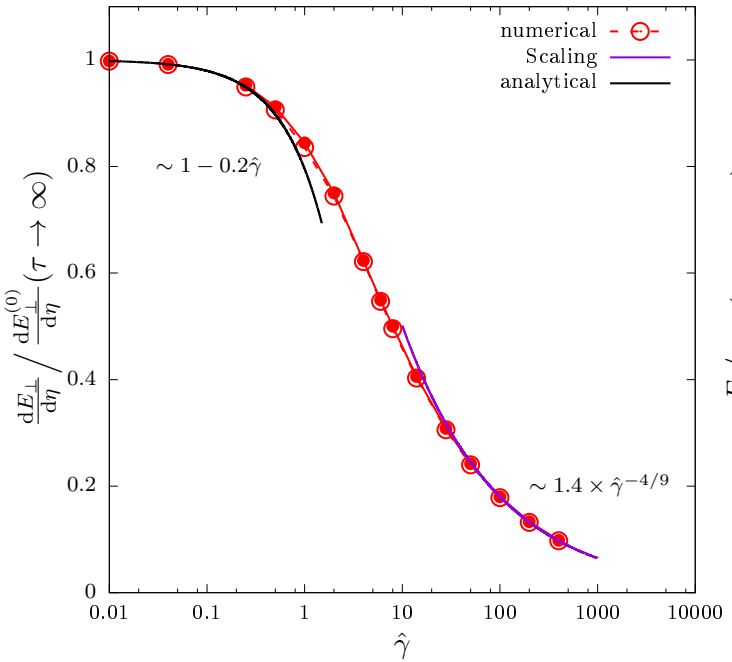

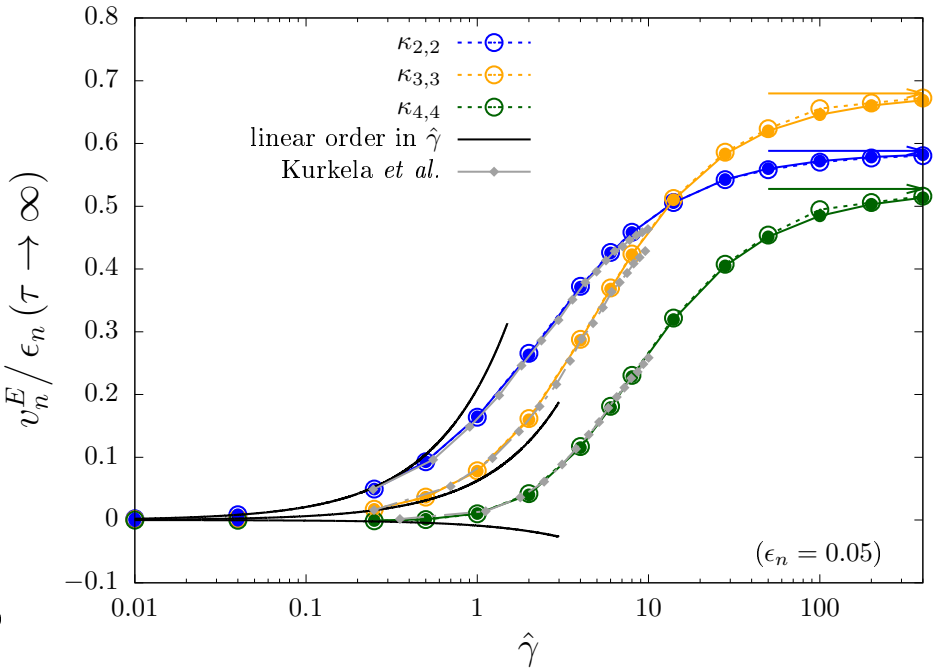

Cooling:

- numerical curve smoothly connects the small-$\hat{\gamma}$ linearized and large-$\hat{\gamma}$ Bjorken scaling results

Anisotropic flow:

- linear order results tangential to numerical curve at small opacities
- agreement with previous results in identical setup

  Kurkela, Taghavi, Wiedemann, Wu PLB 811 (2020) 135901
- saturation at higher $\hat{\gamma}$

$\Rightarrow$ expectation: hydrodynamic behaviour at large opacities

Large Opacity Limit: Hydrodynamics?

- in large opacity regime: should be able to expand in $1/\hat{\gamma}$ similar to Chapman-Enskog method to obtain hydrodynamics from kinetic theory
- **but:** hydrodynamics describes pre-equilibrium stage differently than kinetic theory: free- streaming until $\tau_{\rm eq}/R \sim \hat{\gamma}^{-4/3}$, naively taking $\hat{\gamma} \to \infty$ at fixed τ_0 will cut this out

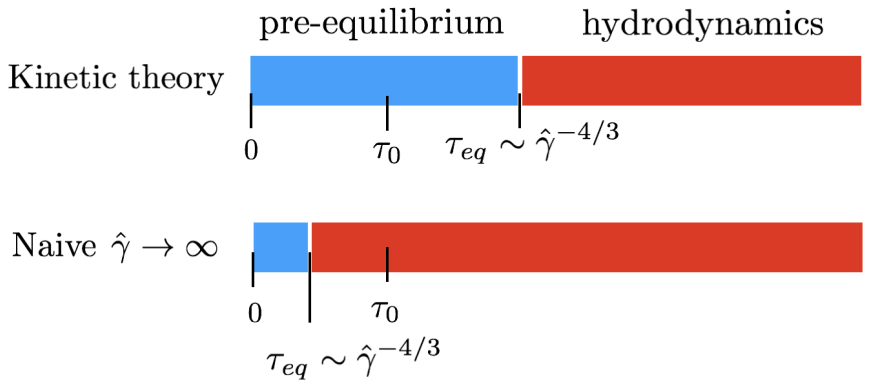

- investigate this by comparing to relativistic viscous hydrodynamics: vHLLE Karpenko, Huovinen, Bleicher Comput. Phys. Commun. 185, 3016 (2014)
- $\hat{\gamma}$ ill-defined for $\tau_0 \to 0 \Rightarrow$ initialize at finite τ_0
- to circumvent particlization disambiguities: compare only observables given in terms of $T^{\mu\nu}$

$$v_2 \sim \epsilon_p = \frac{\int_{\mathbf{x}_\perp} T^{xx} - T^{yy} + 2iT^{xy}}{\int_{\mathbf{x}_\perp} T^{xx} + T^{yy}}\,, \qquad \text{later}: \quad \frac{\mathrm{d}E_\perp}{\mathrm{d}\eta} \sim \frac{dE_{\rm tr}}{d\eta}\tau \int_{\mathbf{x}_\perp} T^{xx} + T^{yy} \tag{6}$$

Non-commutativity of the Limits $\tau_0 \to 0$ and $\hat{\gamma} \to \infty$

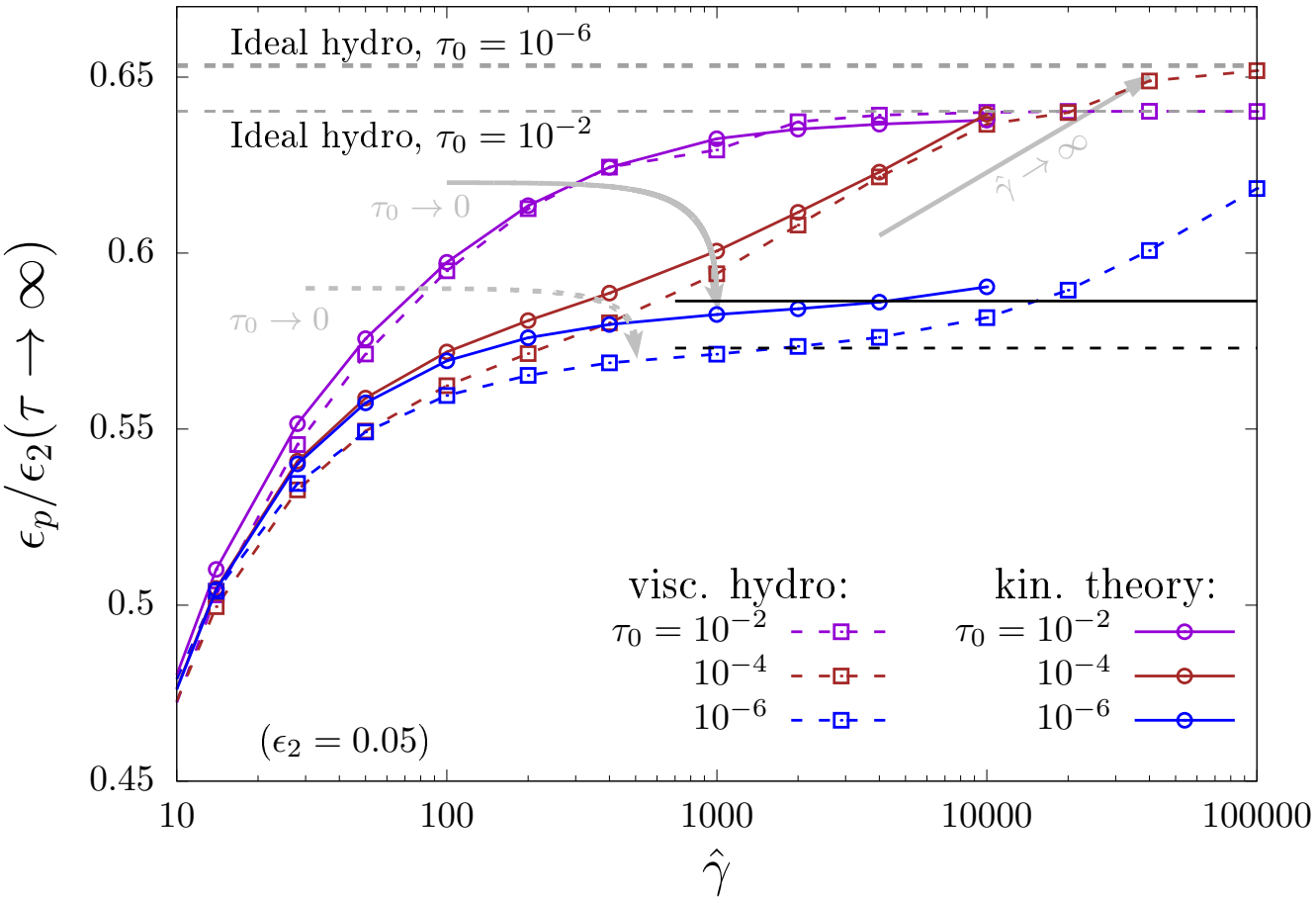

unphysical limit

physical limit

- agreement only for large τ_0: no pre-equilibrium
  - need non-equilibrium description of early time dynamics even at large $\hat{\gamma}$
- curves plateau at physical large-opacity asymptote in the limit $\tau_0 \to 0$
- ideal hydro is the unphysical limit of $\hat{\gamma} \to \infty$ ($\tau_{\mathrm{eq}} \to 0$) at fixed τ_0

$\Rightarrow$ Why is pre-equilibrium important for observables that develop at $\tau \sim R$?

Early time longitudinal cooling

- $\tau \ll R$: local Bjorken flow cooling
  - different early time scaling in different model description

τe in kin. theory

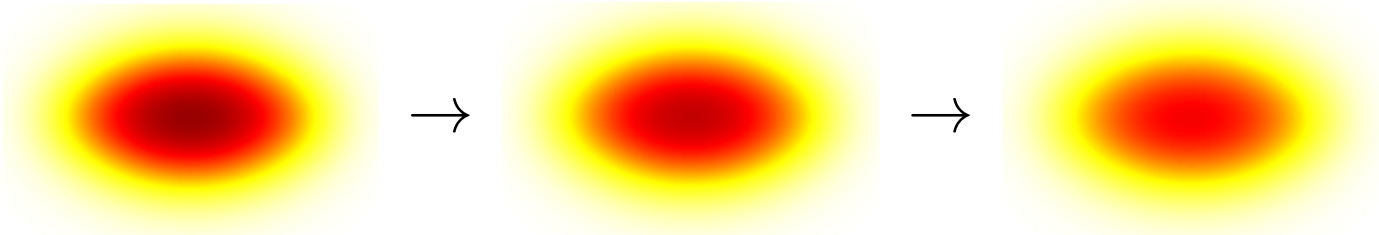

τe in visc. hydro

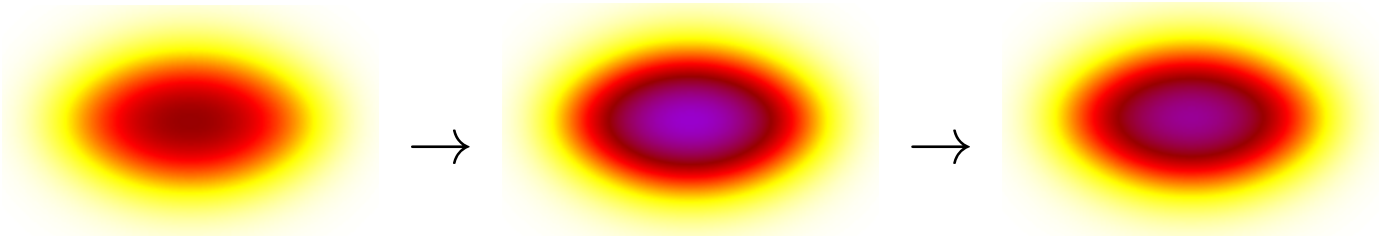

$\tau = 3 \cdot 10^{-6}$fm $\quad$ $\tau = 8 \cdot 10^{-4}$fm $\quad$ $\tau = 3 \cdot 10^{-3}$fm

(times for $4\pi\eta/s = 0.05$)

- dynamics depend on local energy density $\Rightarrow$ inhomogeneous cooling

Eccentricity decrease in inhomogeneous cooling

- reminder: local Bjorken flow cooling at early times follows scaling laws
  - universal attractor curve scaling in the variable $\tilde{w}(\tau, \mathbf{x}_\perp) = \frac{T(\tau,\mathbf{x}_\perp)\tau}{4\pi\eta/s}$

$$\tau^{4/3} e(\tau, \mathbf{x}_\perp) = (4\pi\eta/s)^{4/9} a^{1/9} (\tau\epsilon(\mathbf{x}_\perp))_0^{8/9}\ C_\infty\ \mathcal{E}(\tilde{w}(\tau, \mathbf{x}_\perp)) \tag{7}$$

  - allows to compute semi-analytical prediction of $\epsilon_n(\tau)$ in the absence of transverse expansion

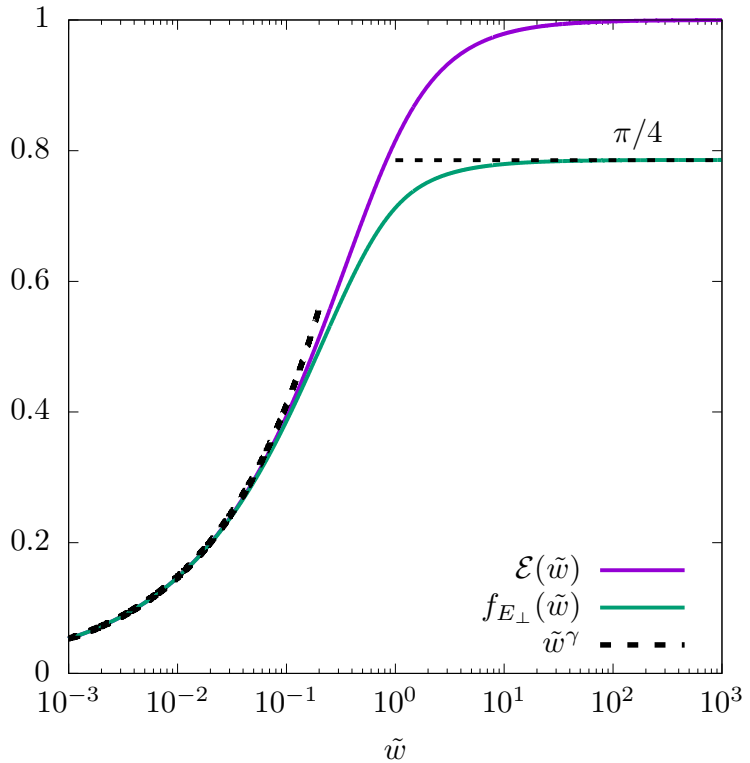

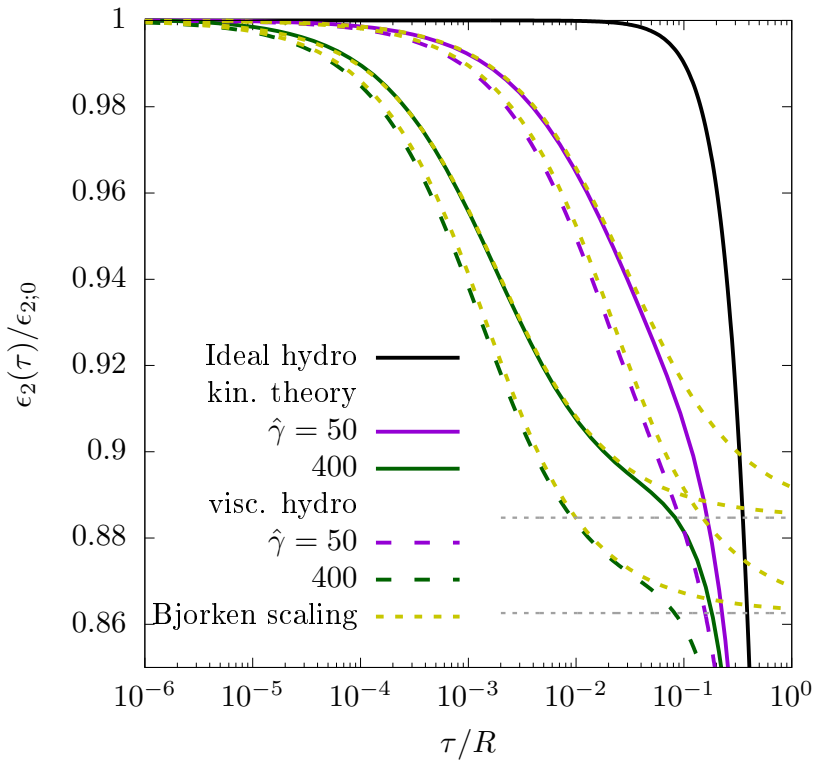

- inhomogeneous cooling changes energy density profile, decreasing eccentricities before transverse flow develops

Improved Hydro Setups

- idea: counteract difference in pre-equilibrium by different hydro initialization
- initialize hydro on its attractor to match Bjorken flow cooling at late times

τe in kin. theory

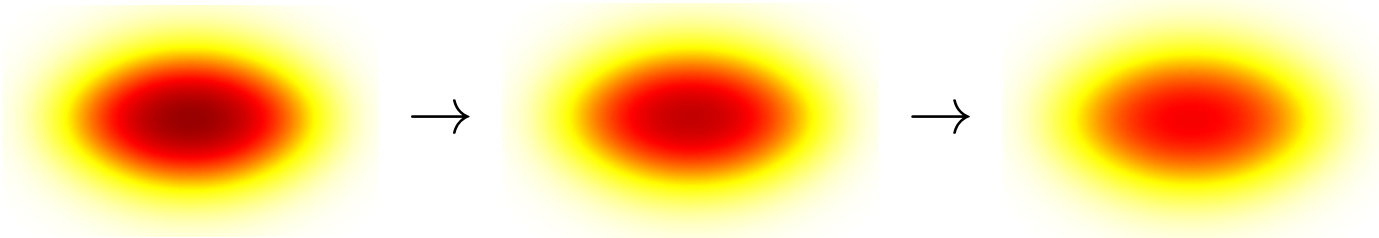

τe in visc. hydro, rescaled e_0

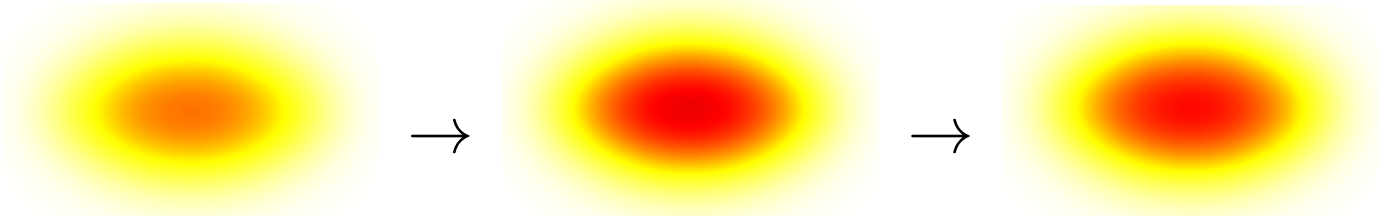

$\tau = 3 \cdot 10^{-6}$fm $\quad$ $\tau = 8 \cdot 10^{-4}$fm $\quad$ $\tau = 3 \cdot 10^{-3}$fm

(times for $4\pi\eta/s = 0.05$)

- more realistic initial condition: average profile (Pb+Pb 30-40%)
  - fixed profile: vary $\hat{\gamma}$ via η/s: $\hat{\gamma} \approx 11 \cdot (4\pi\eta/s)^{-1}$

Initializing on the attractor

- accuracy depends on timescale separation of pre-equilibrium and transv. expansion

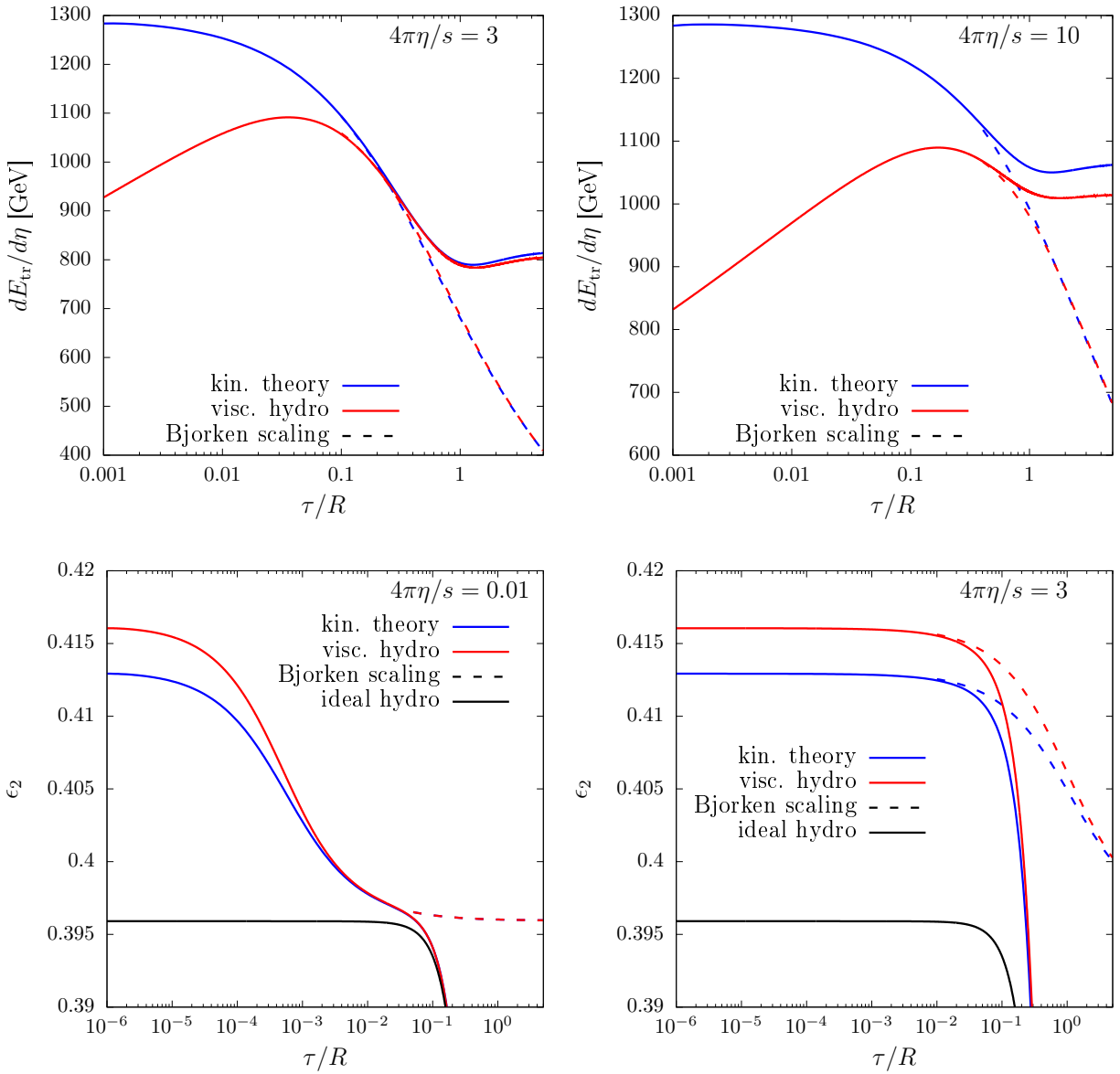

- idea: evolve system in kinetic theory until $\langle \mathrm{Re}^{-1} \rangle_\epsilon$ drops to specific value, then match $T^{\mu\nu}$ to hydro code
- $\mathrm{Re}^{-1} = \frac{\sqrt{6\pi^{\mu\nu}\pi_{\mu\nu}}}{\epsilon}$ measures local shear / deviation from equilibrium
- system immediately starts following similar evolution to a pure hydro run
  - switching too early causes errors in pre-equilibrium
  - results from late switching times more accurate than rescaled hydro
- works just as well with KøMPøST, but with limited range of applicability

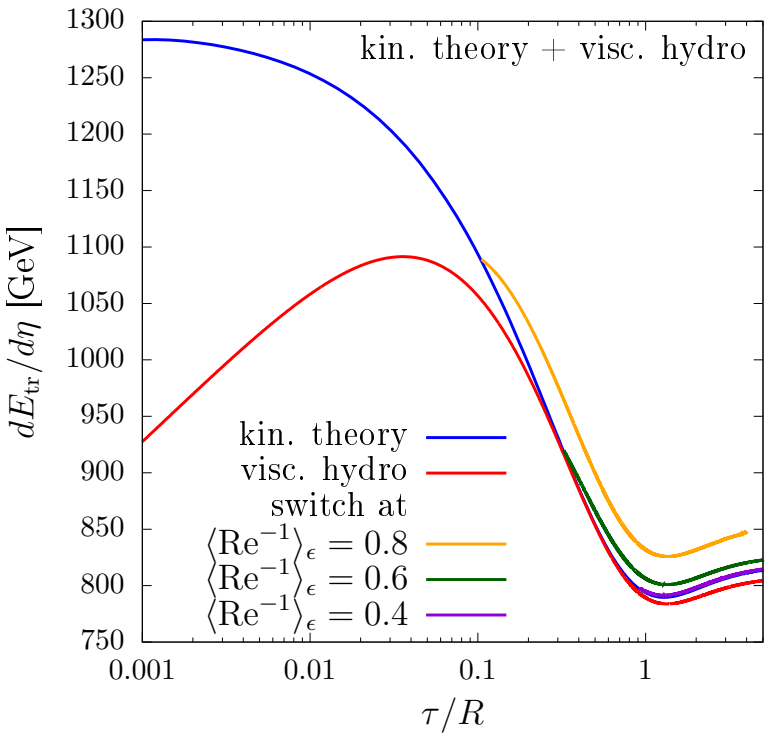

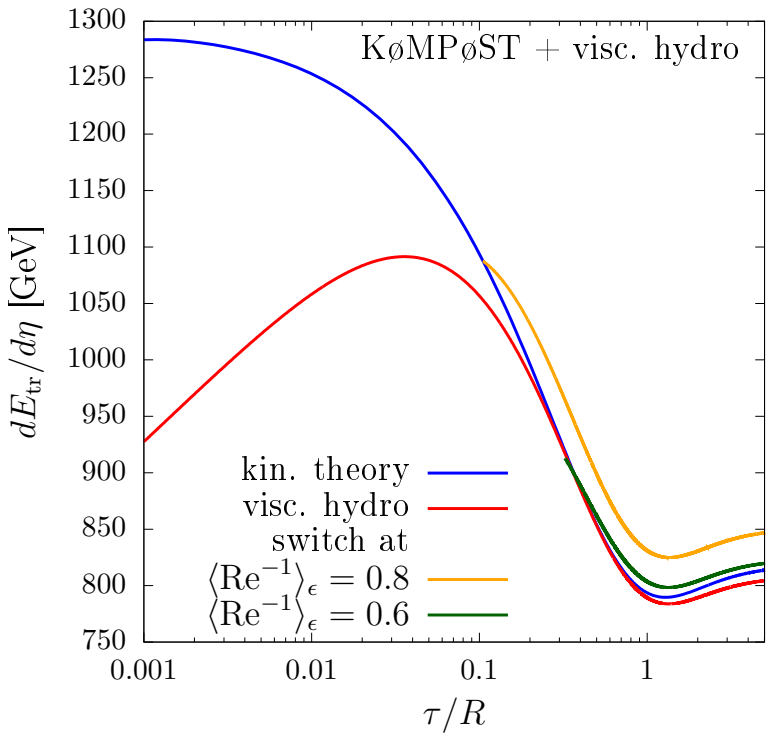

Comparison of the new Hydro schemes with kin. theory

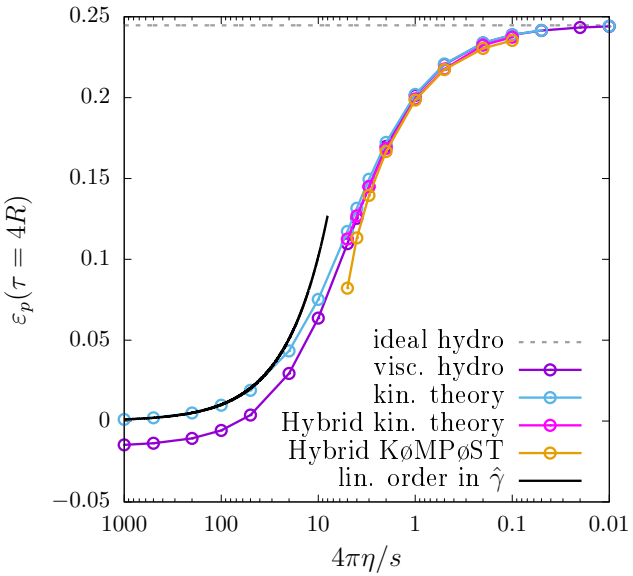

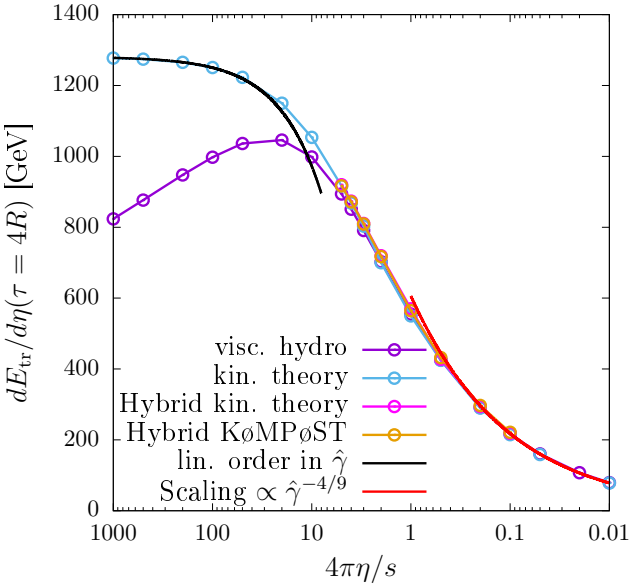

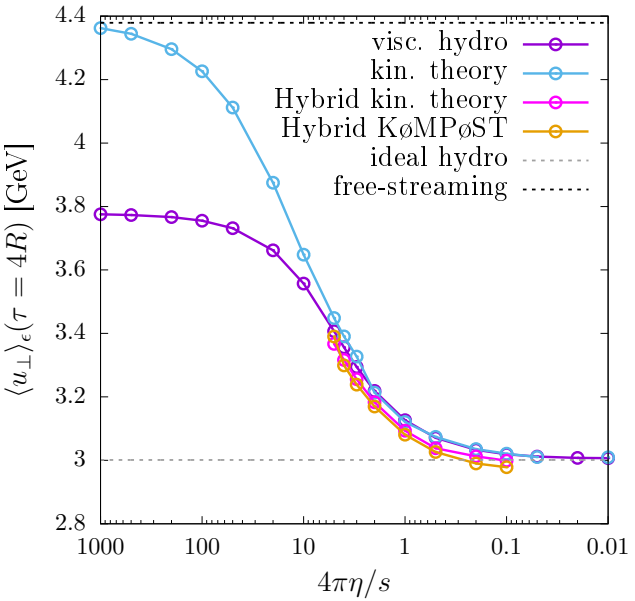

- still good agreement with linear order/free streaming results at small opacities
  - computed (mostly) numerically, since initial condition no longer analytical
- perfect agreement at large $\hat{\gamma}$
- rescaled hydro accurate if $4\pi\eta/s \lesssim 3$ (for Pb+Pb 30-40%)
- Hybrid KøMPøST scheme (here: switching at $\langle \mathrm{Re}^{-1} \rangle_\epsilon = 0.6$) works well for $\frac{E_{\rm tr}}{d\eta}$, slightly underestimates ϵ_p and $\langle u_\perp \rangle_\epsilon$
- Hybrid kin. theory scheme improves ϵ_p, but also underestimates $\langle u_\perp \rangle_\epsilon$

Summary

- kinetic theory description covers full range in opacity from small to large systems
- naive comparison to hydrodynamics: disagreement even at large opacities!
  - difference during pre-equilibrium
  - eccentricity decreases before onset of transverse expansion
  - can be described by universal scaling behaviour of Bjorken flow
- different setup of hydrodynamic simulations can bring agreement at large opacities
  - initializing hydrodynamics on its early-time attractor
  - hybrid models with kinetic theory for pre-equilibrium

Backup

coordinates:

$$\tau = \sqrt{t^2 - z^2} \qquad \eta = \operatorname{artanh}(z/t) \qquad y = \operatorname{artanh}(p_z/E)$$

Boltzmann equation:

$$[\underbrace{p_T \cosh(y-\eta)}_{p^\tau}\partial_\tau + p_\perp^i \partial_i + \underbrace{\frac{p_T}{\tau}\sinh(y-\eta)}_{p^\eta}\partial_\eta] f = C[f]$$

initial condition:

$$f^{(0)}(\tau_0, \mathbf{x}_\perp, \mathbf{p}_\perp, y-\eta) = \frac{(2\pi)^3}{\nu_{\text{eff}}} \frac{\delta(y-\eta)}{\tau_0 p_\perp} F\left(\frac{Q_s(\mathbf{x}_\perp)}{p_\perp}\right)$$

position dependent momentum scale $Q_s(\mathbf{x}_\perp)$ chosen such that

$$\epsilon(\tau_0, \mathbf{x}_\perp) = \frac{\mathrm{d}E_\perp^{(0)}}{\mathrm{d}\eta} \frac{1}{\pi R^2 \tau_0} \exp\left(-\frac{x_\perp^2}{R^2}\right) \left\{1 + \delta_n \left(\frac{x_\perp}{R}\right)^n \exp\left(-\frac{x_\perp^2}{2R^2}\right) \cos[n(\phi_x - \psi_n)]\right\}$$

Solutions in opacity expansion

zeroth order $p^\mu \partial_\mu f^{(0)} = 0$:

$$f^{(0)}(\tau, \mathbf{x}_\perp, \mathbf{p}_\perp, y-\eta) = f^{(0)}\left(\tau_0, \mathbf{x}_\perp - \vec{v}_\perp t(\tau, \tau_0, y-\eta), \mathbf{p}_\perp, \operatorname{arsinh}\left(\frac{\tau}{\tau_0}\sinh(y-\eta)\right)\right)$$

first order $p^\mu \partial_\mu f^{(1)} = C[f^{(0)}]$:

$$f^{(1)}(\tau, \mathbf{x}_\perp, \mathbf{p}_\perp, y-\eta) = \int_{\tau_0}^{\tau} \mathrm{d}\tau' \left(\frac{C[f^{(0)}]}{p^\tau}\right)\left(\tau', \mathbf{x}_\perp{}', \mathbf{p}_\perp, y-\eta'\right)$$

collision kernel: find local rest frame and temperature using Landau matching to compute $C_{RTA}[f^{(0)}] = \frac{p_\mu u^\mu T}{5\,\eta/s}(f_{eq} - f)$ where $f_{eq} = \left[\exp(p_\mu u^\mu/T) - 1\right]^{-1}$

$$T^{\mu\nu} = \nu_{\mathrm{eff}}\tau \int \frac{\mathrm{d}^3 p}{(2\pi)^3 p^\tau} p^\mu p^\nu f^{(0)} \qquad \epsilon u^\mu = u_\nu T^{\nu\mu} \qquad \epsilon = \frac{\nu_{\mathrm{eff}}\pi^2}{30} T^4$$

free-streamed $\delta\epsilon$-cosine:

$$|\mathbf{x}_\perp - \mathbf{v}_\perp \tau|^n \cos(n\phi_{\mathbf{x}_\perp - \mathbf{v}_\perp \tau}) = \sum_{j=0}^{n} \binom{n}{j} x_\perp^{n-j} (-\tau)^j \cos[n\phi_{\mathbf{x}_\perp} + j(\phi_{\mathbf{x}_\perp} - \phi_{\mathbf{v}_\perp})]$$

extract momentum distribution and compute its moments

- jacobian from milne coordinates

$$\frac{\mathrm{d}N}{\mathrm{d}^2p_\perp \mathrm{d}y}(\tau) = \nu_{\mathrm{eff}} \int \mathrm{d}^2x_\perp \, \mathrm{d}\eta \; \tau \, p^\tau \; f(\tau, \mathbf{x}_\perp, \eta, \mathbf{p}_\perp, y)$$

- extract relevant moments; flow harmonics $v_n(p_T)$ in terms of weighted p_T-averages:

$$V_{m,n} = \int \mathrm{d}^2p_T \; p_T^m e^{in\phi_p} \frac{\mathrm{d}N}{\mathrm{d}^2p_T \mathrm{d}y} \qquad v_n^{(m)} = \frac{V_{m,n}}{V_{m,0}}$$

$$\Rightarrow V_{mn}^{(1)}(\tau) = \int_{\mathbf{p}_\perp} e^{in\phi_p} \, p_\perp^m \int_{\mathbf{x}_\perp} \int \mathrm{d}\eta \int_{\tau_0}^{\tau} \mathrm{d}\tau' \; \tau' \frac{\nu_{\mathrm{eff}}}{(2\pi)^3} \frac{p_\mu u^\mu}{\tau_R} (f_{eq} - f)$$

- in total: 6d integral over $\tau', \mathbf{x}_\perp, \eta, \mathbf{p}_\perp$. 4 computed analytically, 2 numerically

$$\underbrace{V_{mn}^{(1,0)}}_{\text{decay of } f^{(0)}} = -\hat{\gamma}\delta_n V_{m0}^{(0)} \; \mathcal{P}_{mn}(\tilde{\tau}) \qquad \underbrace{V_{mn}^{(1,eq)}}_{\text{buildup of } f_{eq}} = +\hat{\gamma}\delta_n \nu_{\mathrm{eff}} R^{-m} \left(\nu_{\mathrm{eff}}^{-1} \frac{\mathrm{d}E_\perp^{(0)}}{\mathrm{d}\eta} R \right)^{\frac{m+3}{4}} \mathcal{Q}_{mn}(\tilde{\tau}) \quad (8)$$

$$\mathcal{P}_{m0}(\tilde{\tau}) = \frac{(m+2)}{3} \int_{\tilde{\tau}_0}^{\tilde{\tau}} \mathrm{d}\tilde{\tau}' \int_0^\infty \mathrm{d}\tilde{x}_\perp \; \tilde{x}_\perp \tilde{T} \, \gamma \exp\left[-\frac{(m+2)}{3} (\Delta\tilde{\tau}'^2 + \tilde{x}_\perp^2) \right] \left[I_0\left(\frac{2m+4}{3} b \right) - \beta I_0'\left(\frac{2m+4}{3} b \right) \right]$$

$$\mathcal{Q}_m(\tilde{\tau}) = \left(\frac{\pi^2}{30} \right)^{-(m+3)/4} \frac{1}{2\pi^{1/2}} \Gamma(m+3) \, \zeta(m+3) \frac{\Gamma\left(\frac{m+2}{2} \right)}{\Gamma\left(\frac{m+3}{2} \right)} \int_{\tilde{\tau}_0}^{\tilde{\tau}} \mathrm{d}\tilde{\tau}' \int_0^\infty \mathrm{d}\tilde{x}_\perp \; \tilde{x}_\perp \tilde{\tau}' \, \tilde{T}^{m+4} \gamma^{-m-2}$$

$$\times \; {}_2F_1\left(\frac{m+2}{2}, \frac{m+2}{2}; 1; \beta^2 \right)$$

- Definition of the moments

$$C_l^m = \int \frac{\mathrm{d}^2 p_\perp \, \mathrm{d}p_\eta}{(2\pi)^3} p^\tau Y_l^m(\theta_p, \phi_p) f$$

  - $Y_l^m(\theta_p, \phi_p)$: spherical harmonics
  - ϕ_p: azimuthal momentum angle
  - θ_p defined by $\cos\theta_p = \frac{p_\eta}{\tau p^\tau}$; dispersion relation $p^\tau = \sqrt{p_\perp^2 + p_\eta^2/\tau^2}$

$$\partial_\tau (p^\tau f) = f \partial_\tau p^\tau - p^i \partial_i f + \frac{p^\mu u_\mu}{\tau_R}(f_{eq} - f)$$

- taking moments: $p^1 = p_\perp \cos\phi_p$, $p^2 = p_\perp \sin\phi_p$, $p_\perp = p^\tau \sin\theta_p$, $p_\eta = \tau p^\tau \cos\theta_p$ together with $Y_l^m(\theta_p, \phi_p)$ result in linear combination of $Y_{l'}^{m'}(\theta_p, \phi_p)$

$$\Rightarrow \partial_\tau C_l^m = \sum_{l',m'} (b_{ll'}^{mm'} + c_{ll'}^{mm'} \partial_1 + d_{ll'}^{mm'} \partial_2 + e_{ll'}^{mm'}(u^\mu)) C_{l'}^{m'} + E_l^m(u^\mu, T)$$

- E_l^m are the moments of the equilibrium term $\frac{p_\mu U^\mu}{\tau_R} f_{eq}$

$$\partial_\tau C_l^m = \sum_{l',m'} (b_{ll'}^{mm'} + c_{ll'}^{mm'}\,\partial_1 + d_{ll'}^{mm'}\,\partial_2 + e_{ll'}^{mm'}(u^\mu))C_{l'}^{m'} + E_l^m(u^\mu, T)$$

Computation:

- $C[f]$ local $\Rightarrow$ change of C_l^m due to blue and purple terms can be computed for each $\mathbf{x}_\perp$-site individually
- red term needs nonlocal discretization of derivative $\Rightarrow$ treated separately in Fourier space
- time evolution via Runge-Kutta-algorithm with time step $0.01\,\min(\tau, \mathrm{R})$
- typical parameters
  - $\mathbf{x}_\perp$ lattice size 256x256
  - Lattice spacing chosen such that the total lattice has size $16R$
  - $l_{\max} = 32$
  - initial time $\tau_0 = 10^{-6}R$

- First, we introduce the reduced distribution $\mathcal{F}_{\mathrm{RLB}}$ via

$$\mathcal{F}_{\mathrm{RLB}} = \frac{\pi \nu_{\mathrm{eff}} R^2 \tau_0}{(2\pi)^3} \left(\frac{\mathrm{d}E_{\perp}^{(0)}}{\mathrm{d}\eta} \right)^{-1} \int_0^{\infty} \mathrm{d}p^{\tau} \, (p^{\tau})^3, \tag{9}$$

such that the Boltzmann eq. becomes

$$\left(\frac{\partial}{\partial \bar{\tau}} + \mathbf{v}_{\perp} \cdot \overline{\nabla} + \frac{1+v_z^2}{\tau} \right) \mathcal{F}_{\mathrm{RLB}} - \frac{1}{\bar{\tau}} \frac{\partial [v_z (1-v_z^2) \mathcal{F}_{\mathrm{RLB}}]}{\partial v_z} = -\hat{\gamma} (v^{\mu} u_{\mu}) \overline{T} (\mathcal{F}_{\mathrm{RLB}} - \mathcal{F}_{\mathrm{RLB}}^{eq}), \tag{10}$$

with

$$\bar{\tau} = \frac{\tau}{\tau_0^{1/4} R^{3/4}}, \qquad \bar{\mathbf{x}}_{\perp} = \frac{\mathbf{x}_{\perp}}{\tau_0^{1/4} R^{3/4}}, \qquad \bar{\epsilon} = \frac{\tau_0 \pi R^2 \epsilon}{dE_{\perp}^{(0)}/d\eta}, \qquad \overline{T} = \left(\frac{\tau_0 \pi R^2 \frac{\pi^2}{30} \nu_{\mathrm{eff}}}{dE_{\perp}^{(0)}/d\eta} \right)^{1/4} T. \tag{11}$$

- Time stepping $\partial_{\tau} \mathcal{F}_{\mathrm{RLB}} = L[\mathcal{F}_{\mathrm{RLB}}]$ performed using RK-3 with 2 intermediate stages.
- Advection performed in an upwind-biased manner using finite differences,

$$c_1 \left(\frac{\partial \mathcal{F}}{\partial x_1} \right)_{s,r} = \frac{\mathbb{F}_{s+\frac{1}{2},r} - \mathbb{F}_{s-\frac{1}{2},r}}{\delta x_1}, \tag{12}$$

where the fluxes $\mathbb{F}_{s \pm \frac{1}{2}}$ are computed using the WENO-5 scheme.

- $\phi_p \to \phi_{p;i} = \phi_0 + \frac{2\pi}{Q_{\phi_p}}(j - \frac{1}{2})$ [Mysovskikh trigonometric quadrature]
- $v_z \to v_{z;j} \equiv$ roots of $P_{Q_z}(v_{z;j})$ [Gauss-Legendre quadrature]
- v_z derivative can be obtained by projection onto the Legendre polynomials:

$$\mathcal{F}_{\mathrm{RLB}} = \sum_{\ell=0}^{\infty} \mathcal{F}_{\ell}^{\mathrm{RLB}} P_{\ell}(v_z) \Rightarrow \left[\frac{\partial[v_z(1-v_z^2)\mathcal{F}_{\mathrm{RLB}}]}{\partial v_z}\right] = \int_{-1}^{1} dv_z' \, \mathcal{K}_P(v_z, v_z')\mathcal{F}(v_z'), \tag{13}$$

where

$$\mathcal{K}_P(v_z, v_z') = \sum_{m=1}^{\infty} \frac{m(m+1)}{2} P_m(v_z) \left[\frac{m+2}{2m+3} P_{m+2}(v_z') - \left(\frac{m}{2m-1} - \frac{m+1}{2m+3}\right) P_m(v_z') - \frac{m-1}{2m-1} P_{m-2}(v_z')\right]. \tag{14}$$

- After discretization, we may write

$$\left[\frac{\partial[v_z(1-v_z^2)\mathcal{F}_{\mathrm{RLB}}]}{\partial v_z}\right]_{ji} = \sum_{j'=1}^{Q_z} \mathcal{K}_{j,j'}^{P} \mathcal{F}_{j'i}^{\mathrm{RLB}}, \tag{15}$$

where the $Q_z \times Q_z$ matrix $\mathcal{P}_{j,j'}$ can be computed before runtime.

Small $\hat{\gamma}$: Free-streaming coordinates

- At small $\hat{\gamma}$, it is convenient to employ the following free-streaming coordinates to parametrise the momentum space:

$$
\begin{aligned}
p^{\tau}_{\mathrm{fs}} &= p^{\tau}\,\Delta, & v_z^{\mathrm{fs}} &= \frac{\tau v_z}{\tau_0 \Delta}, & \Delta &= \sqrt{1+\left(\frac{\tau^2}{\tau_0^2}-1\right)v_z^2},\\
p^{\tau} &= p^{\tau}_{\mathrm{fs}}\,\Delta_{\mathrm{fs}}, & v_z &= \frac{\tau_0 v_z^{\mathrm{fs}}}{\tau \Delta_{\mathrm{fs}}}, & \Delta_{\mathrm{fs}} &= \sqrt{1-\left(1-\frac{\tau_0^2}{\tau^2}\right)v_{z;\mathrm{fs}}^2}.
\end{aligned}
\tag{16}
$$

- Energy-weighted observables can be computed starting from the reduced distribution

$$
\mathcal{F}_{\mathrm{fs}} = \frac{\pi \nu_{\mathrm{eff}} R^2 \tau_0}{(2\pi)^3}\left(\frac{\mathrm{d}E_{\perp}^{(0)}}{\mathrm{d}\eta}\right)^{-1}\int_0^{\infty}\mathrm{d}p^{\tau}_{\mathrm{fs}}\,(p^{\tau}_{\mathrm{fs}})^3 f, \tag{17}
$$

which satisfies

$$
\frac{\partial \mathcal{F}_{\mathrm{fs}}}{\partial \bar{\tau}} + \frac{1}{\Delta_{\mathrm{fs}}}\boldsymbol{v}_{\perp;\mathrm{fs}}\cdot\overline{\nabla}_{\perp}\mathcal{F}_{\mathrm{fs}} = -\hat{\gamma}(v^{\mu}u_{\mu})\overline{T}(\mathcal{F}_{\mathrm{fs}}-\mathcal{F}_{\mathrm{fs}}^{eq}). \tag{18}
$$

- The only change to RLB is that v_z is now discretized in logarithmic scale:

$$
v_{z;j}^{\mathrm{fs}} = \frac{1}{A}\tanh\chi_j, \qquad \chi_j = \left(\frac{2j-1}{Q_z}-1\right)\operatorname{arctanh}A, \tag{19}
$$

where $0 < A < 1$.

- The v_z^{fs} integration is performed using the rectangle method:

$$
\int_{-1}^{1} dv_z^{\mathrm{fs}}\,h(v_z^{\mathrm{fs}}) \to \sum_{j=1}^{Q_z} w_j^{\mathrm{fs}}\,h(v_{z;j}^{\mathrm{fs}}), \qquad w_j^{\mathrm{fs}} = \frac{2\operatorname{arctanh}A}{AQ_z\cosh^2\chi_j}. \tag{20}
$$

Initial conditions: Romatschke-Strickland distribution

- The system is initialized using the Romatschke-Strickland distribution for BE statistics,

$$f_{\rm RS} = \left\{ \exp\left[\frac{1}{\Lambda} \sqrt{(p\cdot u)^2 + \xi_0 (p\cdot \hat{\eta})^2} \right] - 1 \right\}^{-1}, \tag{21}$$

where $\Lambda \equiv \Lambda(\mathbf{x}_\perp)$ satisfies

$$\Lambda^4(\mathbf{x}_\perp) = 2T^4(\tau_0, \mathbf{x}_\perp) \left(\frac{\arctan\sqrt{\xi_0}}{\sqrt{\xi_0}} + \frac{1}{1+\xi_0} \right)^{-1}, \tag{22}$$

- The anisotropy parameter ξ_0 can be used to set $\mathcal{P}_{L;0}/\mathcal{P}_{T;0}$ via

$$\frac{\mathcal{P}_{L;0}}{\mathcal{P}_{T;0}} = \frac{2}{1+\xi_0} \frac{(1+\xi_0)\frac{\arctan\sqrt{\xi_0}}{\sqrt{\xi_0}} - 1}{1 + (\xi_0 - 1)\frac{\arctan\sqrt{\xi_0}}{\sqrt{\xi_0}}}. \tag{23}$$

- $\mathcal{P}_{L;0}/\mathcal{P}_{T;0} = 0$ is achieved when $\xi_0 \to \infty$.
- For $\hat{\gamma} \geq 2$ (RLB), we used $\xi_0 = 20$ ($\mathcal{P}_L/\mathcal{P}_T =$);
- For $\hat{\gamma} \leq 2$ (FS), we used $\xi_0 = 100$ ($\mathcal{P}_L/\mathcal{P}_T =$).
- For both RLB and FS, we have

$$\mathcal{F}^{\rm RS}_{\rm RLB} = \mathcal{F}^{\rm RS}_{\rm fs} = \frac{\bar{\epsilon}/2\pi}{(1+\xi_0 v_z^2)^2} \left(\frac{\arctan\sqrt{\xi_0}}{\sqrt{\xi_0}} + \frac{1}{1+\xi_0} \right)^{-1}. \tag{24}$$

Early Time Bjorken Scaling

Bjorken flow universal attractor curve in scaling variable $\tilde{w}(\tau, \mathbf{x}_\perp) = \frac{T(\tau,\mathbf{x}_\perp)\tau}{4\pi\eta/s}$:

$$\epsilon(\tau)\tau^{4/3} = (4\pi\eta/s)^{4/9} a^{1/9} (\epsilon\tau)_0^{8/9}\; C_\infty\; \mathcal{E}(\tilde{w})\;,$$

$$\tau^{1/3}\frac{\mathrm{d}E_\perp}{d^2\mathbf{x}_\perp \mathrm{d}\eta} = (4\pi\eta/s)^{4/9} a^{1/9} (\epsilon\tau)_0^{8/9}\; C_\infty\; f_{E_\perp}(\tilde{w})$$

- using $\epsilon = aT^4$, recast first eq. into self consistency eq. for $\tilde{w}$
- use this togehter with initial cond. for $\epsilon\tau$ to relate differentials of $\mathrm{d}\tilde{w}$ and $\mathrm{d}x_\perp$
- integrate second equation to find scaling of $\mathrm{d}E_\perp/\mathrm{d}\eta$
- use $\frac{(4\pi\eta/s)^4 a}{dE_\perp^0/d\eta\; R} = \frac{1}{\pi}\left(\frac{4\pi}{5\hat{\gamma}}\right)^4$ to identify $\hat{\gamma}$

$$\frac{dE_\perp/d\eta}{dE_\perp^0/d\eta} = \frac{9}{2}\left(\frac{4\pi}{5\hat{\gamma}}\right)^4\left(\frac{R}{\tau}\right)^3 \int_0^{\tilde{w}(\tau,\mathbf{x}_\perp=0)} \frac{\tilde{w}^3 d\tilde{w}}{\mathcal{E}(\tilde{w})}\left[1 - \frac{\tilde{w}}{4}\frac{\mathcal{E}'(\tilde{w})}{\mathcal{E}(\tilde{w})}\right] f_{E_\perp}(\tilde{w})\;,$$

$$\tilde{w}(\tau, \mathbf{x}_\perp = 0) = \left(\frac{5\hat{\gamma}}{4\pi}\right)^{8/9}\left(\frac{\tau}{R}\right)^{2/3}[C_\infty \mathcal{E}(\tilde{w})]^{1/4}$$

Limits of this scaling law:

- $\hat{\gamma}\left(\frac{\tau}{R}\right)^{3/4} \ll 1 \Rightarrow \tilde{w} \ll 1 \;\Rightarrow\; \mathcal{E}(\tilde{w}) \approx f_{E_\perp}(\tilde{w}) \approx C_\infty^{-1}\tilde{w}^{4/9} \;\Rightarrow\; \frac{dE_\perp/d\eta}{dE_\perp^0/d\eta} = 1$
- $\hat{\gamma}^{3/4}\left(\frac{\tau}{R}\right) \gg 1 \;\Rightarrow\; \tilde{w} \gg 1 \;\Rightarrow\; \mathcal{E}(\tilde{w}) \approx 1, f_{E_\perp} \approx \frac{\pi}{4}$
  $\Rightarrow\; \frac{dE_\perp/d\eta}{dE_\perp^0/d\eta} = \frac{9\pi}{32}\left(\frac{4\pi}{5\hat{\gamma}}\right)^{4/9}\left(\frac{R}{\tau}\right)^{1/3} C_\infty$

$$\epsilon_p = \frac{\int_{\mathbf{x}_\perp} \left(T^{11} - T^{22} + 2iT^{12}\right)}{\int_{\mathbf{x}_\perp} \left(T^{11} + T^{22}\right)} = \frac{\int_{\mathbf{x}_\perp} \int \frac{\mathrm{d}^3 p}{(2\pi)^3}\, p^\tau \left(1 - v_z^2\right) e^{2i\phi_p}\, f}{\int_{\mathbf{x}_\perp} \int \frac{\mathrm{d}^3 p}{(2\pi)^3}\, p^\tau \left(1 - v_z^2\right) f}$$

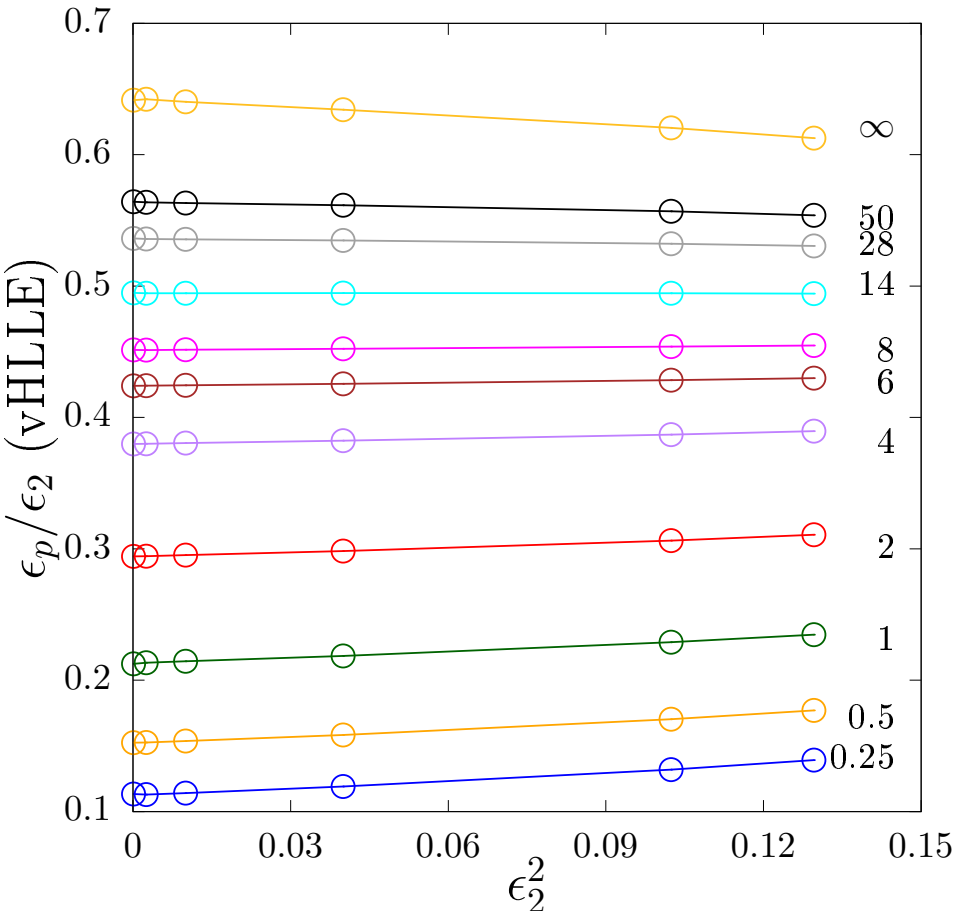

- similar to kinetic results: almost constant, negative trend at large opacities

Eccentricity Evolution in pre-equilibrium Period

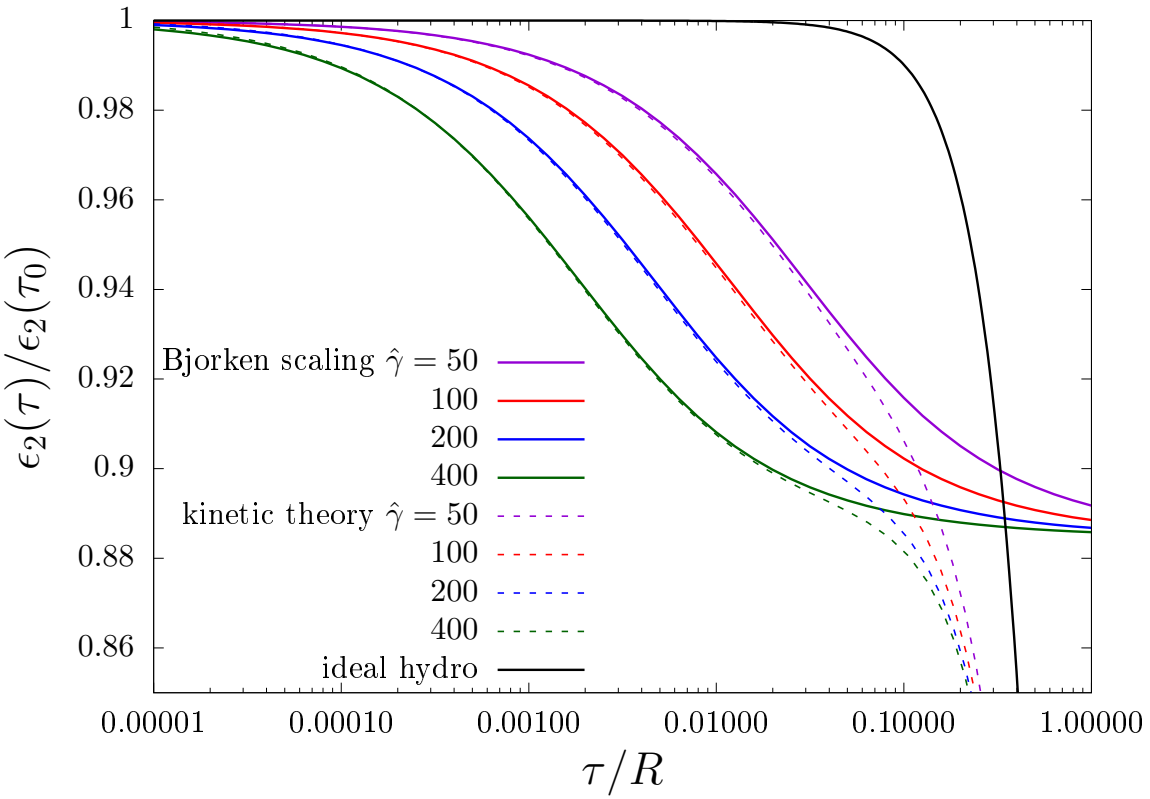

- due to inhomogeneous cooling, eccentricity decays in pre-equilibrium phase
- normalization with ϵ_2 at onset of transverse expansion brings kin. th. results into agreement with ideal hydro